

Effect of Radiant Energy on Near-Surface Water

Binghua Chai, Hyok Yoo, and Gerald H. Pollack*

Department of Bioengineering, Box 355061, University of Washington, Seattle, Washington 98195

Received: August 24, 2009

While recent research on interfacial water has focused mainly on the few interfacial layers adjacent to the solid boundary, century-old studies have extensively shown that macroscopic domains of liquids near interfaces acquire features different from the bulk. Interest in these long-range effects has been rekindled by recent observations showing that colloidal and molecular solutes are excluded from extensive regions next to many hydrophilic surfaces [Zheng and Pollack *Phys. Rev. E* 2003, 68, 031408]. Studies of these aqueous “exclusion zones” reveal a more ordered phase than bulk water, with local charge separation between the exclusion zones and the regions beyond [Zheng et al. *Colloid Interface Sci.* 2006, 127, 19; Zheng and Pollack *Water and the Cell: Solute exclusion and potential distribution near hydrophilic surfaces*; Springer: Netherlands, 2006; pp 165–174], here confirmed using pH measurements. The main question, however, is where the energy for building these charged, low-entropy zones might come from. It is shown that radiant energy profoundly expands these zones in a reversible, wavelength-dependent manner. It appears that incident radiant energy may be stored in the water as entropy loss and charge separation.

Introduction

For many years and from many old studies, it has been known that liquids behave differently from bulk in the region of interfaces. A summary of this older evidence can be found in a comprehensive review written more than a half-century ago by Henniker.¹ Henniker cites more than 100 papers showing that, for many liquids, the physical chemical behavior in the regions near interfaces diverges from the physical chemical behavior farther away, the near-surface liquid taking on different structural forms. Among the cited studies are those of Hardy,² who emphasized structural differences extending up to hundreds of micrometers from the surface. Included among the liquids cited to show such structural differences was water.

By and large, however, the existence and putative functional roles of these extensive interfacial zones have been forgotten. This has been at least partly due to technological advances that have permitted exploration of the few water layers closest to the material surface, which have confirmed the presence of icelike layers.^{3–5} Because of the compelling nature of these observations, the field’s emphasis has focused on those intimate layers, while interest in possible long-range effects, not addressed by those methods, has dwindled.

A notable exception is the work of Green and Otori,⁶ which considered whether such long-range effects might be responsible for the biological phenomenon known as the “unstirred layer”. Surrounding many biological tissues is a zone of extremely slow diffusion extending up to hundreds of micrometers from the surface.⁷ Postulating some role of extended near-surface water, Green and Otori exposed biological tissues and gels to microsphere suspensions and found that the microspheres were excluded from regions on the order of 200 to 300 μm from the respective surfaces, speculating that some feature of near-surface water might be different and might thereby account for the slow diffusion.

* To whom correspondence is addressed. E-mail: ghp@u.washington.edu.
Tel.: (206)685-1880. Fax: (206)685-3300.

More recently, a series of systematic studies confirmed and extended these observations. The first experiments largely duplicated those of Green and Otori (which had been unknown to the authors at the time) with different surfaces. Thus, aqueous microsphere suspensions were exposed to hydrophilic gel surfaces, and the microspheres were excluded from zones extending 100–200 μm from the respective surfaces. Multiple controls were tested for possible artifacts, and all results were negative for artifact or trivial explanations.⁸

Subsequent studies confirmed profound exclusion of microspheres from a series of hydrophilic surfaces and went on to show that it was not only microspheres that were excluded but also various small molecules; hence, the zone of exclusion, labeled hereafter as the “exclusion zone” or EZ, appeared to behave much like an ordered liquid that broadly excluded many molecules.⁹ By various physical chemical methods, this zone was further shown to be both more stable and more ordered than bulk water, albeit less ordered than the icelike zones of the first few layers immediately adjacent to the surface.⁹ (An example of such an EZ is shown below in Figure 2A.)

A notable feature of the EZ is its negative charge. Microelectrodes placed within the zone showed large potential differences relative to the water lying beyond, as high as 100–200 mV negative.¹⁰ Since the potential difference is reckoned between contiguous water regions, the result implies charge separation within the water, and the question arises as to where the energy might come from for driving such charge separation and increased ordering. The fact that the more ordered zone is as large as it is implies that substantial energy might be required, well beyond that available from ordinary surface energy. The question of energy source is the focus of the studies reported here.

Materials and Methods

Sample Preparation. The hydrophilic substances used in the experiments included Nafion tubing (TT-050 with 0.042 in. diameter, Perma Pure LLC) and Nafion 117 per-fluorinated membrane (0.007 in. thick, Aldrich). Before use, they were

immersed in deionized water for 10 min. All experiments were carried out at 22–23 °C and in a dark room to minimize background noise.

All experiments used deionized water, which was obtained from a NANOpure Diamond ultrapure water system. The purity of water from this system is certified by a resistivity value up to 18.2 mΩ·cm, which exceeds ASTM, CAP, and NCCLS type I water requirements. In addition, the deionized water was passed through a 0.2-μm hollow fiber filter for ensuring bacteria- and particle-free water.

Polybead carboxylate microspheres (2.65% solids-latex, Polysciences Inc.), hydrophilic silica microspheres (SiO_2 , Polysciences Inc.), and sulfate microspheres (2.65% solids-latex, Polysciences Inc.) were used to delineate the extent of the exclusion zone. The volume fractions of these aqueous microsphere suspensions were set to 1 to 500.

pH Measurements. Two types of pH measurement were carried out: one using miniature pH probes for tracking the time course of pH change at various distances from the Nafion surface; and another for measuring the pH distribution as a function of distance from the Nafion surface.

For the former, a micro pH probe (catalog no.: PHR-146U, Lazar Research Laboratories, Inc., Los Angeles, CA) connected to a standard pH meter (catalog no.: 6230N, Jenco, San Diego, CA) was used to measure local pH. A 1-cm-high chamber was built with floor dimension 1 cm × 4 cm. The floor was fully covered by a sheet of Nafion. Distilled, deionized water (5 mL) was added slowly enough to avoid disturbing the Nafion sheet. The pH probe was then lowered to the desired height (1, 5, or 10 mm above the sheet), and pH readings were taken at 5 s intervals.

For the pH-dye experiments, a thin 75 mm × 1 mm Nafion film (Sigma Aldrich, Inc.) was first cut and glued at the base of a chamber made out of standard microscope slides. The glass chamber had a 75 mm × 1 mm base and height of 25 mm. Standard pH dye (Sigma Aldrich) was then diluted per manufacturer's recommendation and poured slowly into the chamber. The local pH change next to Nafion was recorded using a charge coupled device (CCD) camera (Scion Corporation) and image.

Effects of Radiant Energy. A Zeiss Axiovert-35 microscope was used for all observations. A high-resolution single chip color digital camera (CFW-1310C), well-suited for bright-field and low-light color video microscopy, as well as for photo documentation was used for color imaging. It has a pixel resolution of 1360 × 1024 with a dynamic range of 10 bits. The CCD sensor of that camera employs the widely used Bayer color-filter arrangement.

Two types of chamber were used. The first was made using a thin cover glass stuck to the bottom of a 1-mm thick cover slide with a 9-mm circular hole in the center; that chamber was used for experiments with Nafion tubing. The second was the same except that the hole was a rectangle of length 3.15 cm × width 1.2 cm × height 1.5 mm, which was for experiments with Nafion membrane, secured with a “microvessel” clip to stand up in the middle of the chamber (0.75 × 4-mm jaws, World Precision Instruments).

Light Source and Incident Power Measurement. For sample illumination, a series of LEDs were used. Infrared LEDs (Gistopics) came in TO-18 packages with parabolic reflectors for reducing the beam-divergence angle. For the visible range, the LED Φ5 series (Nichia) was used. And, for illumination in the UV region, we used LED NSHU590 (Nichia) emitting at 365 nm, and LEDs UVTOP 265 and UVTOP 295 (Sensor

Electronic Technology) encapsulated in metal-glass TO-39 packages with UV-transparent hemispherical lens optical windows, emitting, respectively, at 270 and 300 nm. All LEDs were driven at 2 kHz by a Model D-31 LED driver (Gistopics). Output power was regulated for consistency using a Newport 1815-C optical power meter with Newport 818-UV, 818-SL, and 818-IR probes.

To obtain an incident beam of small diameter, a pinhole 50 μm in diameter and 0.25 mm thickness (Edmund Optics) was used. An integrated holder was built to keep the pinhole and LED together as a single unit, the LED positioned as close as possible to the pinhole. In order to maximize incident power, the unit almost touched the chamber's edge.

Temperature Measurements. To measure the temperature at various points within the chamber, an OMEGAETTE datalogger thermometer HH306 with compact transition ground-junction probe (TJC36 series) was used. This is a compact dual-input thermometer whose stainless steel-sheathed probe is small enough (250 μm) to fit within the EZ. Its range extends from −200 to 1370 °C ± 0.2% and its resolution is 0.1 °C. The datalogger can store up to 16 000 records at programmed intervals as short as once per second.

Results

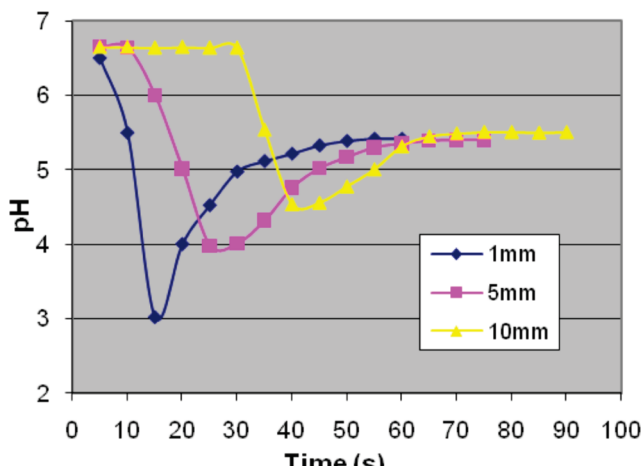
Initial experiments followed earlier studies^{8–10} showing a negatively charged EZ. A lingering question was whether the negative charges of the EZ might be balanced by complementary positive charges beyond the EZ, namely by protons or hydrogen ions.

To explore this possibility, the time course of pH change in the vicinity of Nafion was measured. Figure 1A shows that as the EZ was built, the pH in the zone beyond went sharply downward; it then recovered to a value lower than the initial value. Farther from the Nafion surface, the phasic downturn began later. The results implied a wave of protons emerging from the direction of the EZ, leaving the water at lower pH than prior to the time the EZ had begun building.

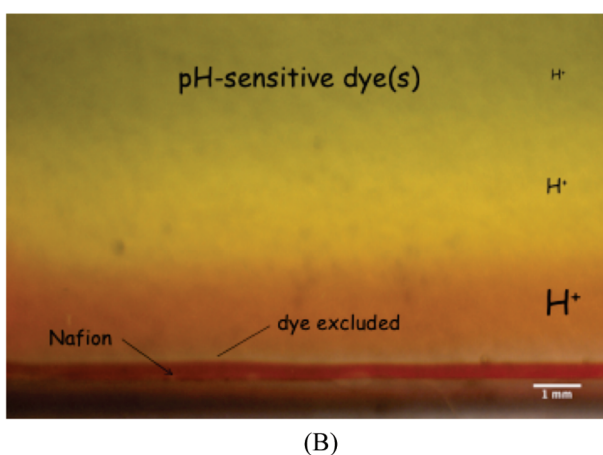
To confirm and extend these pH measurements to longer distances, pH-sensitive dyes were added, and the results are shown in Figure 1B. The clear zone just above the Nafion surface implies that the pH-sensitive dyes are excluded from the EZ. Beyond the EZ, the color is red-orange, indicating a pH less than 3. Farther from the Nafion, the pH was lower than the Nafion-absent control, and eventually, at 10 mm from the Nafion surface and beyond, pH values were similar to controls. Hence, the results imply that the zone beyond the EZ is indeed populated by abundant protons that appear to be associated with EZ buildup.

A clue for the source of energy for EZ buildup came after having inadvertently left the experimental chamber on the microscope stage overnight. The EZ size had diminished overnight; but after turning on the microscope lamp to full intensity, the EZ size began to increase, restoring itself within minutes to its former size, ~300 μm. With preliminary evidence that light could expand the EZ, we investigated systematically whether the energetic source for EZ buildup might indeed be radiant energy.

Liquid water absorbs strongly at wavelengths of 2.9–3.25 μm, which corresponds to the fundamental O–H stretching mode.^{11–13} In this spectral range, the most accessible commercially available source was an LED radiating at 3.1 μm with full width at half-maximum (fwhm) of 0.55 μm; hence, the first light source used was LED31-PR.



(A)



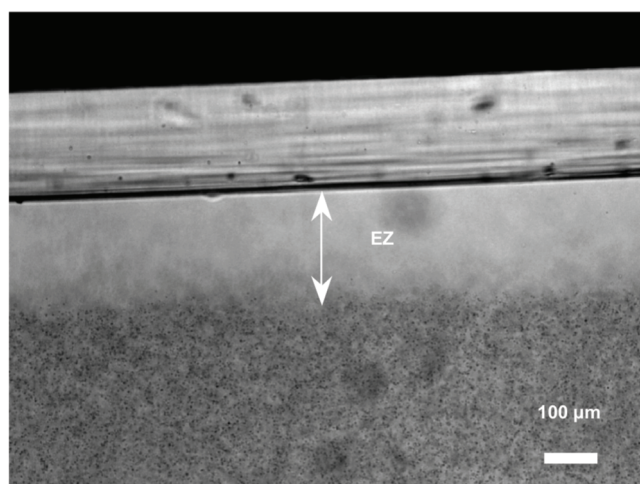
(B)

Figure 1. (A) Time course of pH change following addition of water to Nafion sheet. Values of pH were measured at 5 s intervals using a miniature pH probe positioned at three distances from the Nafion surface, as indicated in the legend. A wave of protons is generated as the EZ forms, giving lower pH. At a distance of 1 mm, the pH drop transiently exceeds 3 pH units, which represents a H^+ increase in excess of 1000 times. (B) Chamber containing Nafion tube (bottom) filled with water containing pH-sensitive dye. The view is normal to the wide face of a narrow chamber. The image obtained 5 min after dye-containing solution was added to Nafion. The red color indicates $pH < 3$; the colors above indicate progressively higher pH levels, with near neutrality at the top.

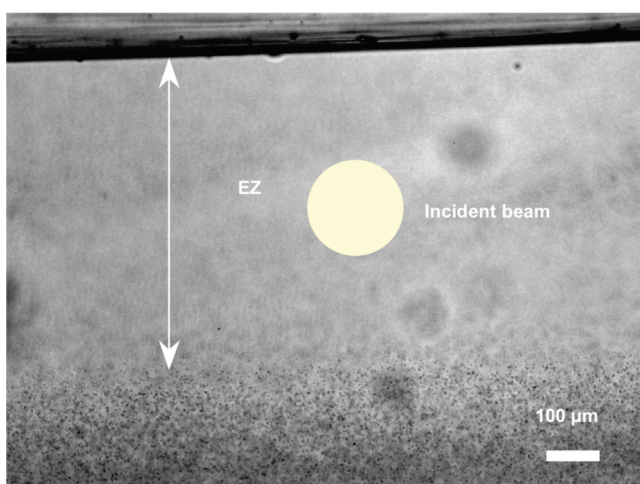
Nafion tubing was suffused with a 1- μ m carboxylate-microsphere suspension with a 1:500 volume fraction, to a depth of ~ 1 mm. The chamber was made using a thin cover glass stuck to the bottom of a 1-mm thick cover slide with a 9-mm circular hole cut in the center and was placed on the stage of the microscope. A pinhole was used to obtain an incident beam of restricted diameter. A fabricated holder integrated the pinhole and LED into a single unit with the LED mounted close to the pinhole. The LED–pinhole axis was vertically oriented.

Basic Observations. The baseline EZ size was first established before measuring IR-induced EZ expansion. The sample was prepared and initially left in the dark. Once enough time had passed for the EZ to stabilize, approximately 5 min, the microscope lamp was turned on briefly to take photomicrographs showing the baseline EZ size. The EZ size after IR irradiation was compared to this baseline size to compute the expansion ratio in each run.

To minimize any effects of microscope illumination on EZ size, the microscope lamp was turned on only when necessary



(A)



(B)

Figure 2. EZ in control experiment (A) and after 5 min of exposure to light from LED31-PR (B). EZ denotes the region in which microspheres are absent. The approximate size of the incident beam is shown in panel B.

for visualizing the EZ, and then immediately turned off. A green filter with a sharp peak at 550 nm was used to further minimize incident radiation. Immediately following the baseline measurements, the incident IR source was turned on. Optical power output was 33 μ W, and the estimated power incident on the sample through the pinhole was ~ 2.4 nW. After 5 min of exposure, the IR LED assembly was removed and the EZ was immediately photographed through the microscope. From the representative records shown in Figure 2, it is apparent that even with modest IR exposure, the EZ grew to approximately three times its control size.

Aware of the potential for contamination by even brief microscope-light illumination, appropriate controls were carried out. The sample was left for 5 min with and without the microscope light turned on. The intensity of incident light was kept the same as in all other experiments, including the green filter. The EZ size was 280 ± 24.1 μ m with light and 260 ± 13.3 μ m without ($n = 5$). Hence, even with microscope illumination of a far longer duration than in actual experiments (5 min vs several seconds), the effect on EZ size was modest. Apparently, the extensive expansion effects observed were due solely to the incident IR radiation.

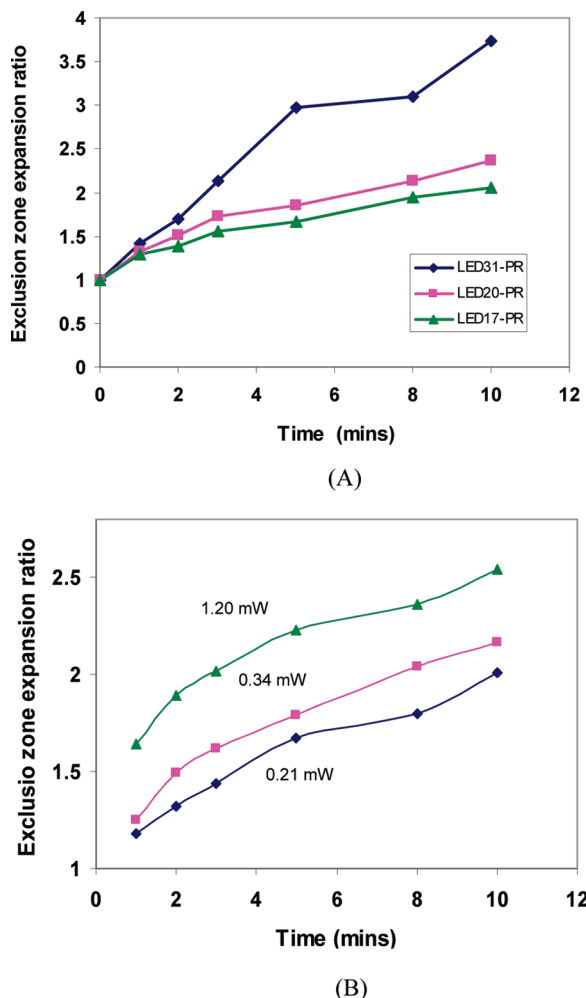


Figure 3. (A) EZ expansion as a function of exposure time, for three IR sources (lower power for LED31-PR). (B) EZ expansion ratios as a function of time during 10 min exposure at different intensities using LED20-PR.

We also tracked the EZ width's time course. This was carried out not only with the 3.1-μm source, but also with the 2.0-μm and 1.75-μm sources (fwhm = 0.16 and 0.18 μm, respectively). For the latter two sources, intensities were maintained at approximately 190 μW; but for the 3.1-μm source, power was kept at the maximally attainable value, 33 μW.

During a 10-min exposure at all three wavelengths, EZs continued to expand approximately linearly (Figure 3A). The largest effect was seen at 3.1 μm, despite lower incident power. To determine whether the EZ continues to expand beyond the 10-min exposure, the 3.1-μm source was left on at the same intensity as above for up to 1 h. The ratios increased from 3.7 ± 0.10 (10 min) to 4.7 ± 0.12 (30 min) and to 6.1 ± 0.17 (1 h), respectively. Hence, the EZ continues to expand with continued exposure for up to at least one hour. Longer durations were deemed unreliable, as evaporation became noticeable; hence measurements were suspended.

Postillumination EZ-size dynamics were examined as well. When the infrared light was turned off after 5 min of exposure, the EZ width remained roughly constant with fluctuations for about 30 min; then, it began decreasing noticeably, reaching halfway to baseline levels in typically ~15 min.

To determine the effect of beam intensity on EZ expansion, the 2-μm source was employed at three power levels, 0.21, 0.34, and 1.20 mW. The rate of EZ expansion increased with an increase of incident power (Figure 3B).

TABLE 1: Temperature Increases Measured at Different Distances from the Nafion Surface after 10 min of Exposure to 3.1-μm Radiation ($n = 3$)

distance from Nafion	mean temperature increase
175 μm	1.1 °C
250 μm	0.91 °C
350 μm	0.92 °C
4 mm	0.91 °C
6 mm	0.92 °C

The results of Figure 3A and B show that, at a given wavelength, EZ expansion is a function of both time and intensity. Hence, EZ growth depends on the cumulative amount of incident energy induced charge separation.

To test whether the expansion might arise out of some unanticipated interaction between the incident radiation and the particular type of microsphere probe, microspheres of different size and composition were tested. For carboxylate microspheres of diameters 0.5, 1, 2, and 4.5 μm at the same volume concentrations (1:500), mean expansion ratios for 5 min of exposure of 3.1-μm radiation were the following: 2.41, 2.97, 3.08, and 3.34, respectively ($n = 6$). For 1-μm microspheres made of carboxylate, sulfate, and silica under conditions the same as above, expansion ratios were 2.97, 3.10, and 1.50. Hence, some material-based and size-based variations are noted—the latter arising possibly because of different numbers of particles per unit volume—but appreciable radiation-induced expansion was nevertheless seen under all circumstances and with all materials. Hence, the existence of the light-induced expansion effect is not material-specific.

We also explored the effect of IR illumination at different depths relative to the water/air interface. Interestingly, EZ expansion was observed well below the water surface. This result is unexpected given the previously reported short penetration depth of IR in water.^{14,15} Nevertheless, IR effects extending far beyond the expected penetration depth have been reported and attributed to coherent energy redistribution of IR-induced excitation of surface layers via pressure waves.^{16,17} A more systematic time-correlated approach will be needed to determine whether any such mechanism might apply here.

Controls for Temperature. Infrared absorption in water causes a temperature elevation. Hence, we considered the possibility that the expansion might arise from an appreciable increase of chamber temperature. To measure local temperatures, an OMEGAETTE datalogger thermometer HH306 was used, with a stainless-steel-sheathed, compact transition ground-junction probe (TJC36 series), small enough (250 μm) to fit within the EZ. With the incident beam positioned to elicit the maximum expansion, i.e., centered 175 μm from the Nafion surface, the measured temperature increases are shown in Table 1. Radiation-induced temperature increases were modest at all positions and fairly uniform over the chamber. We also found little temperature variation with depth, implying that the thermal mass of the probe itself, immersed by varying extents for measurements at varying depths, did not introduce any serious artifact.

Further to this point, we recorded the dynamics of temperature rise. The temperature increase occurred steadily, reaching a plateau of ~1 °C at 10–15 min after turn-on. This plateau was attained at a time that the EZ continued to expand (Figure 3A and associated text). Hence, not only was the temperature increase modest, but also the time course of temperature rise and EZ expansion were not correlated.

Spectral Analysis. A principal objective was to determine EZ-expansion's spectral sensitivity. The experimental setup was

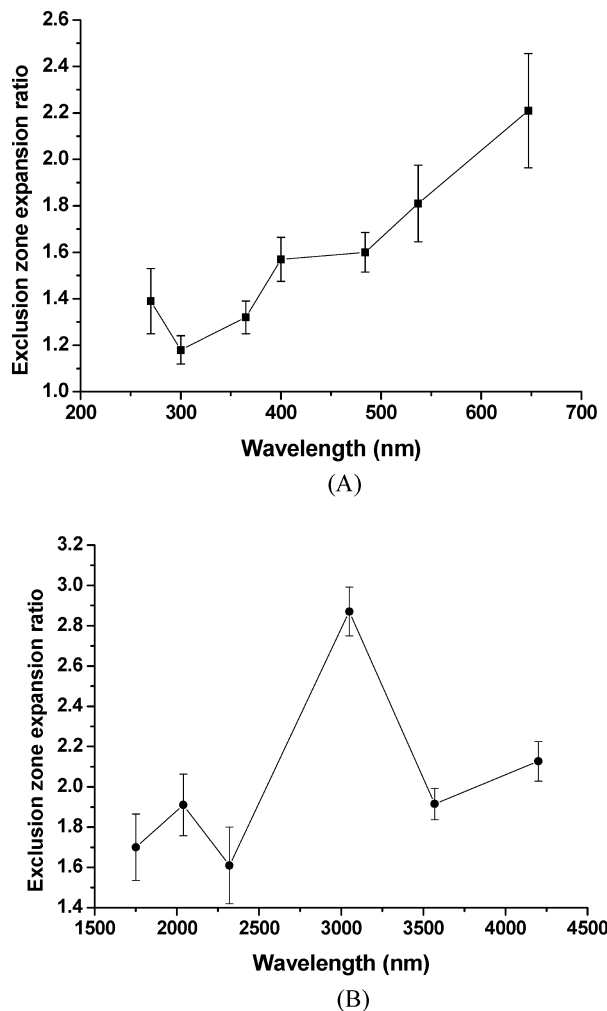


Figure 4. (A) Exclusion-zone expansion ratio under illumination for 5 min in the UV-vis spectral region. (B) Exclusion-zone expansion ratio under illumination for 5 min at IR wavelengths.

similar to that described above. The $\sim 200\text{-}\mu\text{m}$ wide light beam emerging from the pinhole was directed to the middle of EZ, and expansion was measured 300 μm below solution surface. For the UV and visible sources, maintaining consistent optical power output at all wavelengths was achievable within $\pm 10\%$ by adjusting the driver current. But IR sources were considerably weaker; hence, output power was maintained at a lower level, 3 orders of magnitude lower than in the UV-visible ranges. Spectral results are therefore plotted separately.

For UV and visible ranges, all incident wavelengths brought appreciable expansion (Figure 4A). The degree of expansion increased with increasing wavelength, the exception being the data point at 270 nm, which was higher than the local minimum at 300 nm. The higher absorption may reflect the signature absorption peak at 270 nm characteristic of the EZ.¹⁸ Clear wavelength sensitivity was also found in the IR region, the most profound expansion occurring at 3.1 μm (Figure 4B). Recognizing that the optical power available for use in the IR region was 1/600 of that in the visible and UV regions, one can assume that with comparable incident power, the IR curve would shift considerably upward—continuing the upward trend evident in Figure 4A. Hence, the most profound effect is in the mid-IR region, particularly at 3.1 μm .

Discussion

The most significant result of this study is that the near-surface exclusion zone expands extensively in the presence of incident

radiant energy. That is, growth of this more ordered, negatively charged zone is dependent on incident electromagnetic energy.

A secondary result is that growth of this negatively charged zone is associated with buildup of a zone of high proton concentration beyond (Figure 1). Those protons or hydronium ions may facilitate the current flow that can be observed through an external load connected between electrodes placed in the EZ and the zone beyond.¹⁹

Regarding the light-dependent EZ expansion, the overall spectral sensitivity of expansion (Figure 4) follows closely the spectral sensitivity of water absorption. In both cases, there is an overall minimum in the near-UV region, plus a local maximum at 2.0 μm , and a peak in the vicinity of 3.1 μm . If not by coincidence, then a connection is implied between IR absorption and EZ expansion—although the linkage is apparently not through temperature increase, which was both modest and temporally uncorrelated. Further to this point, increasing the bath temperature actually diminishes EZ size (unpublished observations). Hence, the effect of incident electromagnetic energy is apparently nonthermal.

Mechanistic Considerations. One question is how radiant energy could augment EZ size. This question rests on the more basic question of the energy responsible for the original EZ buildup, because buildup and augmentation may be driven from the same energetic source. It is apparent from the data of Figure 4 that mid-IR has a significantly more profound impact than other regions of the spectrum. Since infrared energy is consistently available under ambient conditions, IR energy is likely to be the major agent responsible for both the initial buildup and the augmentation.

To build the EZ, bulk water must undergo some kind of change. We found that as the negatively charged EZ builds, the concentration of protons in the region beyond the EZ likewise builds. Hence, it appears that the mechanism involves radiant energy-induced splitting of bulk water into negative and positive entities. The negative entity forms the ordered EZ, while the positive entity distributes itself broadly over the bulk. The negative-positive combination forms a battery-like entity, fueled by radiant energy.

While the energy of an IR photon is generally considered lower than the dissociation energy of the O-H bond, some dissociation of water occurs even under ambient conditions; i.e., the dissociation constant of water, $K_w = [\text{H}^+][\text{OH}^-]$, underlies all pH measurement, and implies that there is some dissociation even under ambient conditions. Incident IR would merely augment the naturally occurring dissociation. Once dissociated—either through excitation via ambient IR exposure or augmented IR—the negatively charged component would then go on to form the more ordered EZ.

IR-induced reorganization of water is not a new result; IR-induced clathrate formation in liquid water has been reported previously.^{20,21} Another study found an unexpectedly low energy required to delocalize a proton between two neighboring water molecules of liquid water when in the second excited state of O-H stretch vibration; this energy corresponds to less than 20% of the energy for dissociating the water O-H bond in the gas phase.²² Hence, there is precedent for IR-induced molecular rearrangement in liquid water.

The question then becomes: by what mechanism does such ordering take place? Classical thermodynamics prohibits splitting of water by IR due to the low energy of an IR photon. On the other hand, quantum mechanical considerations of liquid water, along with IR and Raman spectra, imply that mid-infrared radiation corresponding to the fundamental OH stretch has

strong resonant effects on water, thereby resonantly exciting the system's vibrational energy. Several studies have reported a vibrational excitation that reorganizes hydrogen-bonded liquid water. These studies show the formation of ion-pair-state ($\text{H}^+ \cdots \text{OH}^-$) water clusters following mid- and near-IR irradiation resonant to the fundamental and fourth harmonic of the O-H stretch.^{16,17,23} Thus, the IR-induced dissociation of water implied here has both precedent and physical rationale, although the exact mechanism is not yet worked out.

In summary, the long-ignored issue of extensive near-surface water ordering may be slightly less enigmatic than thought. The present studies make clear that the buildup of this more ordered near-surface zone involves charge separation and that the underlying energy source is incident radiant energy. Interestingly, the wavelengths most responsible for building this zone are the very wavelengths most strongly absorbed by water. Hence, in a more general context, it may be that a good fraction of the electromagnetic energy absorbed by water is used to build order and separate charge.

Acknowledgment. We thank Drs. H. Ishiwatari and D. Schmidt for technical suggestions, Drs. H. Ishiwatari, B. Liu, R. Stahlberg, and J. Watterson for their comments on the manuscript, and Jeff Magula for building the apparatus. This study was supported by NIH Grants AT-002362 and AR-44813 and ONR Grant N00014-05-1-0773.

References and Notes

- (1) Henniker, J. C. *Rev. Mod. Phys.* **1949**, *21*, 322.
- (2) Hardy, W. B. *Proc. R. Soc. London* **1912**, *86*, 610.
- (3) Yalamanchili, M. R.; Atia, A. A.; Miller, J. D. *Langmuir* **1996**, *12*, 4176.
- (4) Nihonyanagi, S.; Ye, S.; Uosaki, K.; Dreesen, L. *Surf. Sci.* **2004**, *573*, 11.
- (5) Noguchi, H.; Hiroshi, M.; Tominaga, T.; Gong, J. P.; Osada, Y.; Uosaki, K. *Phys. Chem. Chem. Phys.* **2008**, *10*, 4987.
- (6) Green, K.; Otori, T. *J. Physiol.* **1970**, *207*, 93.
- (7) Pollack, G. H.; Clegg, J. *Phase Transitions in Cell Biology: Unexpected linkage between unstirred layers, exclusion zone, and water*; Springer: New York, 2008; pp 143–152.
- (8) Zheng, J.-M.; Pollack, G. H. *Phys. Rev. E* **2003**, *68*, 031408.
- (9) Zheng, J.-M.; Chin, W.-C.; Khijniak, E.; Pollack, G. H. *Adv. Colloid Interface Sci.* **2006**, *127*, 19.
- (10) Zheng, J.-M.; Pollack, G. H. *Water and the Cell: Solute exclusion and potential distribution near hydrophilic surfaces*; Springer: Netherlands, 2006; pp 165–174.
- (11) <http://www.lsbu.ac.uk/water/vibrat.html> (accessed September 24, 2009).
- (12) Venyaminov, S. Y.; Prendergast, F. G. *Anal. Biochem.* **1997**, *248*, 234–245.
- (13) Bertie, J. E.; Ahmed, M. K.; Eysel, H. H. *J. Phys. Chem.* **1989**, *93*, 2210–2218.
- (14) Hale, G. M.; Querry, M. R. *Appl. Opt.* **1973**, *12*, 555.
- (15) Wieliczka, D. M.; Weng, S.; Querry, M. R. *Appl. Opt.* **1989**, *28*, 1714.
- (16) Toyama, N.; Kohno, J.; Kondow, T. *Chem. Lett.* **2006**, *35*, 966–967, No. 8.
- (17) Toyama, N.; Kohno, J. Y.; Kondow, T. *Chem. Phys. Lett.* **2006**, *420*, 77.
- (18) Chai, B.-H.; Zheng, J.-M.; Zhao, Q.; Pollack, G. H. *J. Phys. Chem. A* **2008**, *112*, 2242.
- (19) Pollack, G. H. <http://uwtv.org/programs/displayevent.aspx?rID=22222>, 2008 (accessed September 24, 2009).
- (20) Yokono, T.; Shimokawa, S.; Mizuno, T.; Yokono, M.; Yokokawa, T. *Jpn. J. Appl. Phys.* **2004**, *43*, 1436.
- (21) Shimokawa, S.; Yokono, T.; Yokono, T.; Yokokawa, T.; Arais, T. *Jpn. J. Appl. Phys.* **2007**, *46*, 333.
- (22) Bakker, H. J.; Nienhuys, H.-K. *Science* **2002**, *297* (5581), 587.
- (23) Klochkov, D. V.; Kotkovskil, G. E.; Nalobin, A. S.; Tananina, E. S.; Chistyakov, A. A. *JETP Lett.* **2002**, *75* (1), 22–24.

JP908163W